# Chapter 8

# Phytochemical Investigation of the *Vitex negundo* (L.) Leaves

# 8 Phytochemical Investigation of the *Vitex negundo* (L.) Leaves

## 8.1 Introduction

*Vitex negundo* (Verbenaceae) is an aromatic shrub which thrives in tropical to temperate regions and is native to China, South Asia, East Africa, Japan, Indonesia, and South America [233]. It is rich in complex bioactive components that imparts multifaceted pharmacology thus, making it popular in Ayurveda for the treatment and management of pain and inflammation. The plant is well known for anti-inflammatory, antioxidant, antimicrobial, anti-tumor, anti-androgenic, antihyperglycemic, anti-nociceptive, anti-osteoporotic, hepatoprotective, and insecticidal activities [234, 235]. It is privileged with distinct secondary metabolites such as iridoid glycosides, flavonoids, lignans, and terpenoids. Its two major biomarker metabolites are iridoid glycosides, negundoside and agnuside which make around 2-4% w/w of dried leaves and the pharmacological potential of *Vitex* is primarily attributed to these two [236].

Till now the preclinical pharmacological investigations of *V. negundo* are focused around the iridoid class of molecules, i.e., negundoside and agnuside only [237, 238]. The current study aimed at phytochemical screening of *V. negundo* leaves for other bioactive phytoconstituents, followed by their purification and characterization.

Interestingly, the potent antioxidant activity of the iridoid free fraction, prompted to do detailed phytochemical investigation and led to the isolation of 2,3-Dehydrosilychristin (**7**), a flavonolignan, along with other phytoconstituents. 2,3-Dehydrosilychristin is a silychristin derivative usually found in silymarin, a standardized fruit extract of milk thistle (*Silybum marianum* L.) [239]. Silymarin is enriched with flavonolignans and is well-known for hepatoprotective, immunomodulatory, anti-inflammatory, and antioxidant activities [240]. Chemically, silymarin is a complex mixture of flavonolignans and flavonoid such as silybin (A and B), isosilybin (A and B), silychristin

(A and B), silydianin, and taxifolin (flavonoid) [241]. Despite the studies done on separation and quantification of components of silymarin, detailed flavonolignan profile is still not available. Silybin is reported to be the chief active component (40-65%) of silymarin and is held responsible for hepatoprotective effects and other biological activities [241, 242]. 2,3-Dehydrosilychristin is also one of the minor constituents reported from silymarin [243]. Due to the complexity associated with the complete separation from the silymarin flavonolignans and flavonoids, the bioactive role of other components of silymarin is not known.

This work is the first report of isolation and characterization of 2,3-Dehydrosilychristin (**7**) from any other species beyond the milk thistle. The presence of components of silymarin in *Vitex negundo* could provide a hope to attenuate the pressure on the *Silybum marianum*, as until now it is the only available source of silymarin. The *Vitex negundo* could prove to be an alternative source and hence could prevent the endangering of *Silybum marianum* species which is only limited to Mediterranean region [244]. The discovery of 2,3-Dehydrosilychristin (**7**) from the *Vitex*, opens new avenues to look into iridoid free fraction for potential biomarkers, beyond the conventional iridoid biomarkers of *Nirgundi*.

## 8.2 Experimental section

### 8.2.1 General experimental procedure

As mentioned in Section 4.2.7.1.

### 8.2.2 Plant material

The plant material of *Vitex negundo* (Nirgundi leaves) was collected and authenticated by Dr. Sanjeev Kumar. A specimen sample (accession number: DG/22-23/555) was preserved in Museum of Department of Dravyaguna at the Faculty of Ayurveda, Institute of Medical Sciences, Banaras Hindu University, Varanasi, India.

### 8.2.3 Extraction and isolation

1 kg of dried and powdered leaves were extracted by cold percolation method using ethanol-water (8:2) with intermittent stirring. The cycle was repeated 3-4 times to ensure complete extraction. The extract was concentrated till dried and was further diluted with 200 ml distilled water and subjected to partitioning with an equal volume of hexane for defatting. The aqueous layer was then passed through the celite filter to remove the particulate matter and again diluted with 200 ml of distilled water. The aqueous layer was further diluted with distilled water and loaded over the preactivated HP20 resin to adsorb the organic compounds from the water stream. The adsorbed material was eluted with the increasing concentration of methanol in water. The initial fraction (fr 1 or spent) was ignored as it mainly contained the water-soluble salts, sugars and highly water-soluble components. Different fractions were collected with increasing concentration of methanol, the fractions were then subjected to repeated purification for isolation of different phytoconstituents and were characterized using NMR and mass spectral data [245].

**Gardenin B** (**4**): 1H NMR (500 MHz, $CDCl_3$) $\delta$ 7.91 (d, $J$ = 8.6 Hz, 2H), 7.02 (d, $J$ = 8.6 Hz, 2H), 6.62 (s, 1H), 4.00 (s, 3H), 3.99 (s, 3H), 3.97 (s, 3H), 3.80 (s, 3H). 13C NMR (126 MHz, $CDCl_3$) $\delta$ 178.9, 161.7, 158.7, 156.0, 152.8, 152.3, 138.7, 132.3, 130.1, 122.8, 114.1, 106.6, 90.3, 60.9, 60.1, 56.3, 55.4. HRMS *m/z*: $[M+H]^+$ calc. 359.1125, obs. 359.1139 [246].

**Butin** (**5**): 1H NMR (500 MHz, $CD_3OD$) $\delta$ 7.70 (d, $J$ = 9.2 Hz, 1H), 7.01 (d, $J$ = 0.9 Hz, 1H), 6.86 (dd, $J$ = 9.2, 2.2 Hz, 1H), 6.83 (d, $J$ = 9.0 Hz, 1H), 6.49 (dd, $J$ = 9.2, 2.2 Hz, 1H), 6.31 (d, $J$ = 2.2 Hz, 1H), 5.45 (dd, $J$ = 7.1, 4.3 Hz, 1H), 3.13 (dd, $J$ = 16.7, 4.2 Hz, 1H), 2.89 (dd, $J$ = 16.9, 7.0 Hz, 1H). 13C NMR (125 MHz, $CD_3OD$) $\delta$ 191.2, 165.2,

164.9, 145.8, 145.5, 131.9, 129.2, 118.3, 115.4, 114.9, 114.4, 112.9, 103.1, 78.8, 44.2. HRMS *m/z*: $[M+H]^+$ calc. 273.0757, obs. 273.0749 [247].

**Luteolin** (**6**): 1H NMR (500 MHz, $CD_3OD$) $\delta$ 7.45 – 7.39 (m, 2H), 6.89 (d, $J$ = 9.5 Hz, 1H), 6.53 (d, $J$ = 1.8 Hz, 1H), 6.44 (s, 1H), 6.28 (d, $J$ = 1.8 Hz, 1H). 13C NMR (125 MHz, $CD_3OD$) $\delta$ 182.67, 164.63, 164.24, 161.5, 158.8, 149.8, 146.2, 122.4, 119.6, 115.9, 113.9, 104.6, 104.4, 99.4, 94.7. HRMS *m/z*: $[M+H]^+$ calc. 287.0550, obs. 287.0561 [248].

**2,3-Dehysrosilychristin** (**7**): 1H NMR (500 MHz, DMSO- $d_6$) $\delta$ 12.48 (s, 1H), 10.80 (s, 1H), 9.61 (s, 1H), 9.41 (s, 1H), 9.06 (s, 1H), 7.64 (s, 1H), 7.62 (s, 1H), 6.97 (d, $J$ = 1.6 Hz, 1H), 6.82 (d, $J$ = 10.2 Hz, 1H), 6.78 (d, $J$ = 8.1 Hz, 1H), 6.42 (d, $J$ = 2.0 Hz, 1H), 6.20 (d, $J$ = 2.0 Hz, 1H), 5.56 (d, $J$ = 6.5 Hz, 1H), 5.08 (t, $J$ = 5.3 Hz, 1H), 3.77 (s, 3H), 3.75 – 3.69 (m, 2H), 3.57 (q, $J$ = 6.1 Hz, 1H). 13C NMR (125 MHz, DMSO-$d_6$) $\delta$ 176.3, 164.4, 161.2, 156.6, 149.2, 148.1, 147.3, 147.0, 141.4, 136.3, 132.6, 130.3, 124.2, 119.2, 116.3, 116.0, 115.8, 111.0, 103.5, 98.7, 93.8, 88.0, 63.4, 56.1, 53.4. HRMS *m/z*: $[M+H]^+$ calc. 481.1129, obs. 481.1138 [239].

**Apigenin** (**8**): 1H NMR (500 MHz, DMSO-$d_6$) $\delta$ 7.86 (d, $J$ = 9.0 Hz, 2H), 6.95 (d, $J$ = 9.0 Hz, 2H), 6.73 (s, 1H), 6.53 (d, $J$ = 1.8 Hz, 1H), 6.28 (d, $J$ = 1.8 Hz, 1H). 13C NMR (125 MHz, DMSO-$d_6$) $\delta$ 183.9, 164.6, 164.3, 161.5, 161.5, 159.1, 128.5, 122.9, 116.1, 104.9, 104.1, 99.4, 94.8. HRMS *m/z*: $[M+H]^+$ calc. 271.0601, obs. 271.0613 [249].

**Gallic acid** (**9**): 1H NMR (500 MHz, DMSO- $d_6$) $\delta$ 6.93 (s, 2H). 13C NMR (125 MHz, DMSO-$d_6$) $\delta$ 169.4, 145.7, 139.1, 121.6, 109.8. HRMS *m/z*: $[M+H]^+$ calc. 171.0288, obs. 171.0295 [100].

**Ferulic acid** (**10**): 1H NMR (500 MHz, $CDCl_3$) $\delta$ 7.65 (d, $J$ = 16.3 Hz, 1H), 7.09 (d, $J$ = 1.8 Hz, 1H), 7.00 (dd, $J$ = 8.2, 2.2 Hz, 1H), 6.89 (d, $J$ = 8.4 Hz, 1H), 6.34 (d, $J$ = 16.7 Hz, 1H), 3.86 (s, 3H). 13C NMR (125 MHz, $CDCl_3$) $\delta$ 169.5, 149.4, 149.1, 145.7, 126.6,

123.8, 117.4, 116.0, 113.2, 56.3. HRMS *m/z*: $[M+H]^+$ calc. 195.0652, obs. 195.0641 [250].

**Isoorientin** (**11**): 1H NMR (500 MHz, $CD_3OD$) $\delta$ 7.43 (d, $J$ = 2.4 Hz, 1H), 7.41 (q, $J$ = 2.1 Hz, 1H), 6.89 (d, $J$ = 9.5 Hz, 1H), 6.64 (s, 1H), 6.49 (s, 1H), 5.21 (dt, $J$ = 8.6, 2.6 Hz, 1H), 3.90 – 3.82 (m, 1H), 3.76 (dt, $J$ = 12.1, 4.6 Hz, 1H), 3.70 – 3.61 (m, 1H), 3.55 – 3.46 (m, 2H), 3.39 – 3.35 (m, 1H). 13C NMR (125 MHz, $CD_3OD$) $\delta$ 182.8, 164.7, 163.9, 160.2, 157.8, 149.8, 146.2, 122.0, 119.6, 115.9, 113.9, 108.8, 104.1, 103.7, 94.3, 81.9, 79.3, 73.9, 71.4, 70.8, 61.8. HRMS *m/z*: $[M+H]^+$ calc. 449.1078, obs. 449.1091 [251].

**Agnuside** (**12**): 1H NMR (500 MHz, DMSO-$d_6$) $\delta$ 7.87 (d, $J$ = 8.8 Hz, 1H), 7.82 – 7.76 (m, 1H), 6.87 (d, $J$ = 8.8 Hz, 1H), 6.83 (d, $J$ = 8.7 Hz, 1H), 6.37 (dd, $J$ = 6.1, 2.0 Hz, 1H), 5.81 (s, 1H), 5.20 – 5.16 (m, 1H), 5.08 (dd, $J$ = 6.1, 3.9 Hz, 1H), 5.02 – 4.94 (m, 1H), 4.87 (dd, $J$ = 8.2, 3.9 Hz, 2H), 4.53 (d, $J$ = 7.8 Hz, 2H), 4.36 (d, $J$ = 5.3 Hz, 1H), 3.66 (d, $J$ = 11.6 Hz, 1H), 3.21 – 2.98 (m, 4H), 2.85 (t, $J$ = 7.6 Hz, 1H). 13C NMR (126 MHz, DMSO-$d_6$) $\delta$ 165.6, 162.5, 140.8, 140.3, 132.7, 132.0, 120.7, 115.9, 105.1, 98.8, 96.2, 81.1, 77.6, 77.1, 73.8, 70.5, 62.5, 61.6, 47.2, 45.3. HRMS *m/z*: $[M+H]^+$ calc. 467.1548, obs. 467.1558 [237, 252].

**Negundoside** (**13**): 1H NMR (500 MHz, $CD_3OD$) $\delta$ 7.86 (d, $J$ = 8.8 Hz, 2H), 7.11 (s, 1H), 6.82 (d, $J$ = 8.7 Hz, 2H), 5.49 (d, $J$ = 2.9 Hz, 1H), 5.00 – 4.93 (m, 2H), 3.96 (d, $J$ = 11.9 Hz, 1H), 3.79 – 3.65 (m, 2H), 3.43 (d, $J$ = 6.1 Hz, 2H), 2.93 (d, $J$ = 4.7 Hz, 1H), 2.23 (dd, $J$ = 9.7, 2.8 Hz, 1H), 2.17 (dd, $J$ = 16.2, 5.6 Hz, 1H), 1.74 – 1.56 (m, 2H), 1.42 (td, $J$ = 13.0, 7.6 Hz, 1H), 1.27 (s, 3H). 13C NMR (126 MHz, $CD_3OD$) $\delta$ 168.6, 165.9, 161.9, 149.8, 131.5, 120.8, 114.7, 112.4, 96.5, 93.7, 78.5, 77.1, 74.7, 73.6, 70.4, 61.4, 51.0, 39.9, 29.8, 28.8, 23.0. HRMS *m/z*: $[M+H]^+$ calc. 497.1654, obs. 497.1663 [237, 253].

**Butrin** (**14**): 1H NMR (500 MHz, DMSO-$d_6$) $\delta$ 7.80 (d, $J$ = 9.0 Hz, 1H), 6.97 (d, $J$ = 2.7 Hz, 1H), 6.91 (dd, $J$ = 7.7, 2.4 Hz, 1H), 6.83 – 6.77 (m, 1H), 6.70 (d, $J$ = 2.3 Hz, 1H),

5.50 (dd, *J* = 6.9, 4.1 Hz, 1H), 5.22 (dt, *J* = 7.3, 2.5 Hz, 1H), 5.04 (dt, *J* = 7.1, 2.4 Hz, 1H), 3.95 – 3.87 (m, 2H), 3.79 – 3.65 (m, 7H), 3.60 – 3.53 (m, 1H), 3.55 – 3.46 (m, 2H), 3.45 – 3.41 (m, 1H), 3.11 (dd, *J* = 16.8, 4.2 Hz, 1H), 2.81 (dd, *J* = 16.8, 7.0 Hz, 1H). 13C NMR (125 MHz, DMSO-$d_6$) $\delta$ 191.2, 166.2, 154.9, 147.6, 145.4, 131.2, 130.5, 128.3, 120.4, 115.5, 115.4, 115.0, 102.4, 101.5, 101.4, 79.1, 77.7, 77.6, 77.4, 77.4, 74.1, 74.1, 71.0, 70.9, 62.0, 61.8, 44.2. HRMS *m/z*: $[M+H]^+$ calc. 597.1814, obs. 597.1827 [254].

### 8.2.4 DPPH (2, 2-diphenyl-1-picrylhydrazyl) assay (free radical scavenging activity)

The antioxidant activity of the extract and isolated compound was determined by measuring their ability to scavenge DPPH, a powder composed of stable free-radical molecules. A 200 µM DPPH solution was prepared in methanol [255]. The concentration of seeds and leaves extract was 2 mg/ml. The isolated compounds were dissolved in methanol to produce a 2.5 mM concentration. Then samples (75 µL) were mixed with DPPH solution (75 µL) and incubated for 30 min at room temperature in a dark place. The absorbance (Ab) of the reaction solution was measured at 517 nm using a UV-visible spectrophotometer. Ascorbic acid was used as a reference and dissolved in methanol to make the solution of 2.5 mM concentration. Methanol and a mixture of methanol (75 µL) and DPPH (75 µL) were used as blank and negative control, respectively. The free radical scavenging activity was calculated according to following formula:

$$Scavenging\ effect(\%) = \frac{Ab517_{control} - Ab517_{sample}}{Ab517_{control}} * 100$$

### 8.2.5 Anti-inflammatory assay

#### 8.2.5.1 Cell culture

The THP-1 human monocyte cells from American Type Culture Collection (ATCC; Manassas, VA) were cultured and differentiated to the macrophage phenotype using PMA (Phorbol myristate acetate).

#### 8.2.5.2 Compound and LPS treatment

The stock solution of compound **7** was prepared in 100% DMSO and diluted in complete culture medium to the final desired concentrations. 0.1% DMSO (v/v) (Sigma-Aldrich, USA) and indomethacin (50 μM concentration) was taken as disease control and positive control, respectively. PMA-differentiated THP-1 macrophages (THP-1 macrophages) were pretreated with varying concentrations of compound **7** (10, 50 and 100 μM or 0.1% DMSO as solvent control) for 2h prior to 4 h stimulation with 10 ng/ml of LPS (Sigma-Aldrich, *E. coli* O111:B4 strain) in medium containing the same concentration of Compound **7** or 0.1% DMSO alone.

#### 8.2.5.3 ELISA: quantification of cytokine proteins

The presence of inflammatory cytokines in culture supernatants was quantified using human cytokine assay kits (R&D Systems; Minneapolis, MN). The procedure was followed as per the manufacturer's instructions. Human TNF-α, IL-6, IL-8, and VEGF Quantikine ELISA kits (R&D Systems) were used according to the manufacturer's protocol.

### 8.2.6 Hepatoprotective activity

#### 8.2.6.1 Animals

Female Swiss albino mice aged 6-7 weeks and weighing 22-26 g were procured from Institute of Medical Sciences, Banaras Hindu University BHU. The animals were housed at standard conditions (23 ± 3 ℃, 45 ± 5% humidity, 12/12 h light/dark cycle), provided water and feed *ad libitum*, and acclimatized for 7 days before experiment. No food but only water was provided 2 h prior to experiment. The experimental protocol was approved by Ethical Committee in Animal Experimentation of IIT (BHU).

#### 8.2.6.2 Experimental design

Mice were divided randomly into 5 experimental groups (*n=7*). Group I was healthy control and received only saline (no hepatotoxicity induction); Group II was hepatotoxicity induced control (single i.p. injection of paracetamol at dose 400 mg/kg) treated with saline; Group III, IV, and V mice were treated with Compound **7** (20 mg/kg), silybin (20 mg/kg, Standard 1), and silymarin (300 mg/kg, Standard 2), respectively for 7 days prior to paracetamol administration. After 24 h of single i.p. injection of paracetamol all the animals were anesthetized using xylazine 2% and ketamine 10%. The blood was drawn from retro-orbital plexus and serum was collected by centrifugation of heparin-treated blood at 10,000 rpm for 15 minutes. The animals were sacrificed by cervical dislocation and abdominally opened to remove livers. The livers were cleaned and further stored in a 10% formalin solution for histopathology analysis.

#### 8.2.6.3 Assessing hepatic injury

Serum samples were used for determining enzymatic activities of aspartate aminotransferase (AST) and alanine aminotransferase (ALT) using commercial kits (Arkray healthcare PVT Ltd, Gujarat, India) and presented as U/L. Serum samples were subjected to lipid profiling (total cholesterol and triglycerides) via enzymatic method and random glucose level determination using hexokinase method. These analysis were done using commercial kits (Arkray healthcare PVT Ltd, Gujarat, India) and presented as mg/dl. For histopathological analysis, the mid-sections of livers (left lobe) were processed using standard methods for light microscopy. The specimens were stained with hematoxylin-eosin dye and examined via microscopy.

### 8.2.7 Statistical analysis

Statistical analysis was performed using GraphPad Prism (Version 5.0). The experiments were performed in quadruplets, results represented in mean ± S.D, and graphs plotted

with mean values and error bars. The statistical difference was analyzed using one-way and two-way analysis of variance (ANOVA) followed by Tukey's test and Pearson correlation. $p < 0.05$ was considered statistically significant.

### 8.2.8 Molecular docking

Molecular docking studies were performed using AutoDock 4.2 to study interactions between Compound **7** and TNF-α (PDB: 7JRA), IL-6 (PDB: 1ALU), IL-8 (PDB: 5D14), VEGF (PDB: 1FLT). The molecular docking protocol is same as mentioned in Section 4.2.3.2.

## 8.3 Result & Discussion

### 8.3.1 Extraction and isolation

The extract was fractionated using HP20 resin using increasing concentration of methanol in water. The initial fraction (fr 1 or spent) was ignored and rest of the adsorbed material was eluted with 150 mL of 25% (fr 2), 50% (fr 3), 75% (fr 4) methanol in water and finally washed with 150 mL of 100% methanol (fr 5). All the fractions were concentrated, lyophilized, and subjected to DPPH antioxidant assay. Fr 2 and 4 showed 50% scavenging activity at 1 mg/mL concentration. Fr 3 showed very potent free radical scavenging activity (100% at 0.5 mg/mL). TLC profiling of all the fraction was carried out with agnuside and it was noticed that in fr 2 some other compounds were also present when visualized by anisaldehyde sulfuric acid reagent.

For detail phytochemical investigations, fr 4 and fr 5 were combined based on TLC profiling and subjected to silica gel column chromatography. The purification yielded some common sterols, lupeol (**1**), ursolic acid (**2**), betulinic acid (**3**) and uncharacterized fatty acids, that were characterized by co-TLC with available standards and 1H NMR spectra. A crystalline, UV active compound was also obtained and characterized as gardenin B (**4**, 14 mg) [246].

The TLC observation of fr 3 revealed several UV active compounds, thus fr 3 was subjected to silica gel column chromatography and eluted with increasing concentration of ethyl acetate in hexane. It yielded various phenolic components after repeated purification that included butin (**5**, 132 mg), luteolin (**6**, 13 mg), 2,3-dehydrosilychristin (**7**, 650 mg), apigenin (**8**, 98 mg), gallic acid (**9,** 10 mg), ferulic acid (**10**, 32 mg), and isoorientin (**11**, 210 mg). Butin and 2,3-dehydrosilychristin is reported for the first time from *V. negundo*. Furthermore, repeated purification of fr 2 led to the isolation of agnuside (**12,** 3 gm), negundoside (**13,** 2.5 gm), butrin (**14,** 200 mg) (Figure 8.1). Butin is an aglycon of butrin, perhaps a product of butrin hydrolysis during the extraction and isolation. The isolated compounds were characterized by comparing their melting point (Appendix, Table A.6), NMR and mass spectra with reported literature [100, 246, 256-262]. The 2,3-dehydrosilychristin was characterized by comparing the 1H and 13C NMR spectra with reported literature and 2D NMR (Appendix, Figure A.39-A.46) [239].

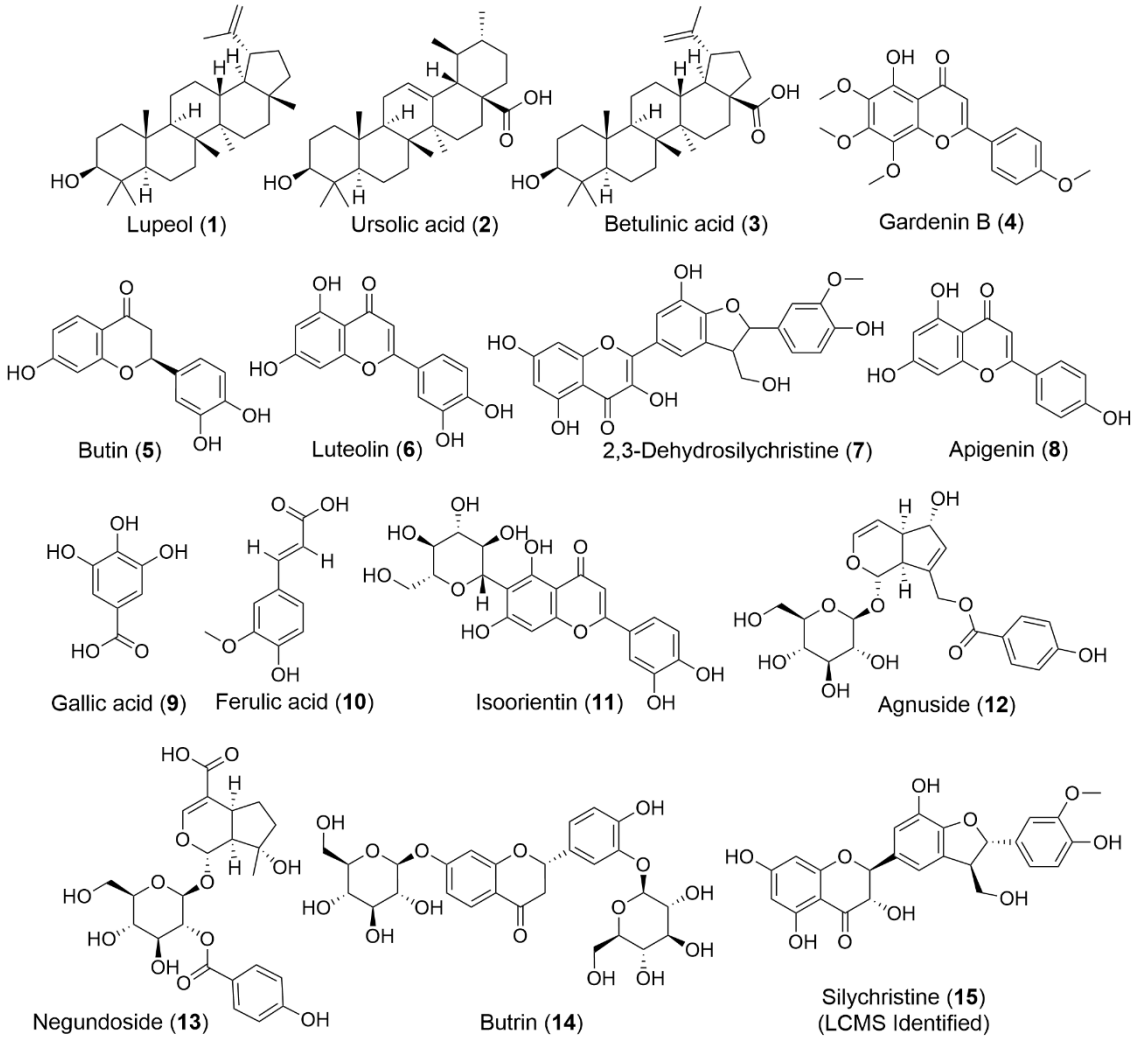


Figure 8.1 Chemical structures of isolated compounds.

### 8.3.2 LC-MS studies

The presence of silychristin in *Vitex* extract was also evaluated via preliminary LC-MS studies and results were compared with the LC-MS profile of silymarin. In the method, extracted ion chromatogram (EIC) of silymarin showed three major peaks at 13.30, 16.25, and 17.30 min corresponding to m/z 481 [M-H] (Appendix, Figure A.47-A.50). The visual inspection of the reported HPLC profile of silymarin revealed the elution pattern of silymarin flavolignans. Silychristin is relatively polar and elutes early at RP18. Based on this observation, the peak at 13.30 min with m/z 481 [M-H] was assigned to silychristin in silymarin chromatogram. This was also supported by literature as various reported silymarin chromatograms on RP 18 mentioned the elution of silychristin first [263]. The

same LC-MS method was used to profile the *V. negundo* leaf extract, and in EIC for mass 481 Da, a peak appeared at 13.30 for m/z 481 [M-H] that confirmed the presence of silychristin in *Vitex* (Appendix, Figure A.51 & A.52).

### 8.3.3 Antioxidant activity

Initially, the leaf extract and fractions of *V. negundo* showed moderate to potent antioxidant activity, hence compound **7** was also evaluated for antioxidant activity. The extracts and compound **7** displayed potent DPPH scavenging activity (Figure 8.2), ranging between 70%-90%. Being a potent antioxidant, compound **7** was further evaluated for anti-inflammatory potential as Ayurveda mentioned Nirgundi for several inflammatory conditions [264, 265].

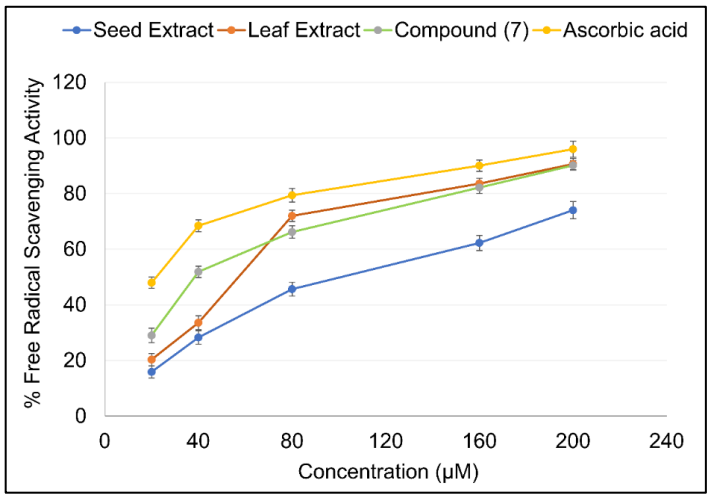


Figure 8.2 Percent free radical scavenging activity of **7**, seed extract, leaf extract of *V. negundo*. All the values are expressed as Mean ± S.D.

### 8.3.4 Anti-inflammatory activity

Several cytokine mediators and mechanisms are involved in inflammation, and some pro-inflammatory mediators include TNF-α, IL-6, and ROS [266]. The other inflammatory mediators gaining importance are IL-8 and VEGF. Besides being an angiogenic factor, VEGF is involved in inflammation as it facilitates the release of inflammatory mediators [267]. IL-8 involves activation of neutrophils, and periodontal disease is one of the

inflammatory conditions mediated by neutrophils. Ayurvedic practice involves the use of Nirgundi in dental care and related periodontal conditions [268]. The unusual presence of compound **7** in *V. negundo* with potent antioxidant activity prompted to perform *in vitro* anti-inflammatory activity. Since NSAIDs are the first line of drugs for inflammatory conditions, indomethacin was used as positive control, and the effect of compound **7** on the secretion of TNF-α, IL-6, IL-8, and VEGF was assessed in THP-1 macrophages.

*In vitro* assay showed that compound **7** displayed better activity even at 10 µM concentration as it reduced cytokine levels compared to disease control (Figure 8.3). At a concentration 10 µM, compound **7** inhibited IL-8 secretion similar to positive control indomethacin (at 50 µM concentration); it inhibited VEGF more prominently than indomethacin, but the inhibition of TNF-α and IL-6 was less than indomethacin. At concentrations 30, 50, and 100 µM, the inhibition of cytokine secretion by compound **7** was better than indomethacin. The inhibition of IL-6, IL-8, and VEGF secretion was approximately similar at both 30 µM and 50 µM concentrations of compound **7** but TNF-α secretion was more suppressed at 50 µM than at 30 µM concentration. Compound **7** at concentration 100 µM showed maximum inhibition of IL-6, IL-8, and VEGF secretion, whilst surprisingly the inhibition of TNF-α was not that prominent compared to 50 µM concentration. Thus, from the *in vitro* activity it was found that compound **7**, even at 30 µM concentration was more effective in inhibiting secretion of inflammatory cytokines than indomethacin at 50 µM. Compound **7** displayed good inhibitory potential against crucial inflammatory cytokines involved in inflammation, and compared to indomethacin, it inhibited these cytokines even at lower concentrations. Hence, compound **7** might be inferred to have role in the anti-inflammatory potential of Nirgundi.

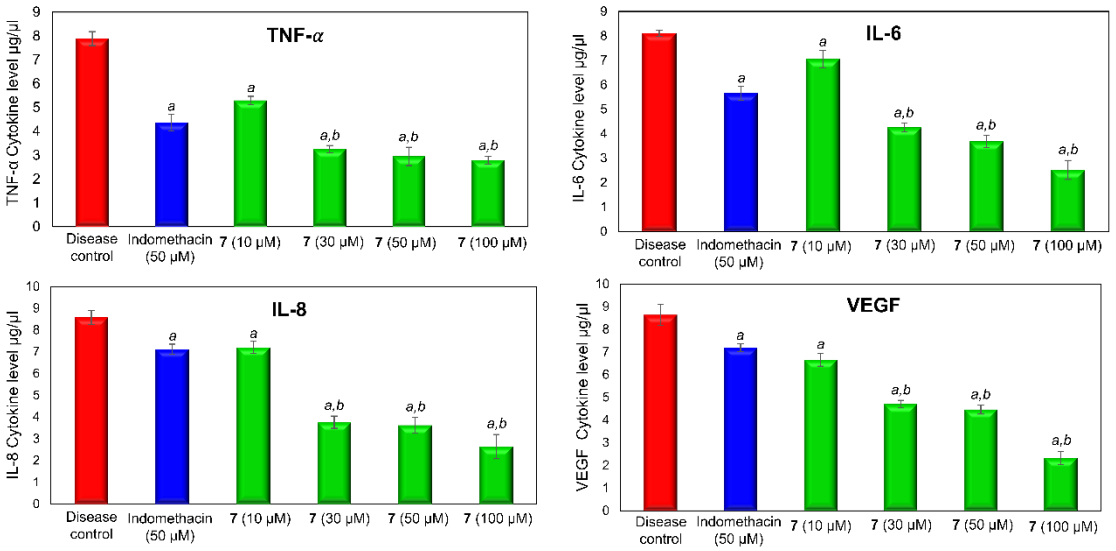


Figure 8.3 Alterations in inflammatory cytokine (TNF-α, IL-6, IL-8, and VEGF) levels post-treatment with **7** at different concentrations. Data expressed in Mean ± S.D; $^{a}p < 0.05$ vs. disease control; $^{b}p < 0.05$ vs. positive control (indomethacin).

### 8.3.5 *In vivo* hepatoprotective studies

Compound **7** was also investigated for hepatoprotective potential via *in vivo* studies in female Swiss albino mice. As serum AST and ALT are the biomarker enzymes for monitoring liver damage, the estimation of these biomarker enzymes in the serum of healthy and test compound-treated mice was conducted. The AST and ALT levels were significantly amplified in Group II compared to that in Group I. The serum AST and ALT levels were reduced drastically in Group III compared to Group II and were approximately equivalent to those in Group I. The serum AST and ALT levels fell to the normal range in Groups IV and V. The statistical analysis displayed significant differences in AST and ALT levels in Group III, Group IV, and Group V (Figure 8.4).

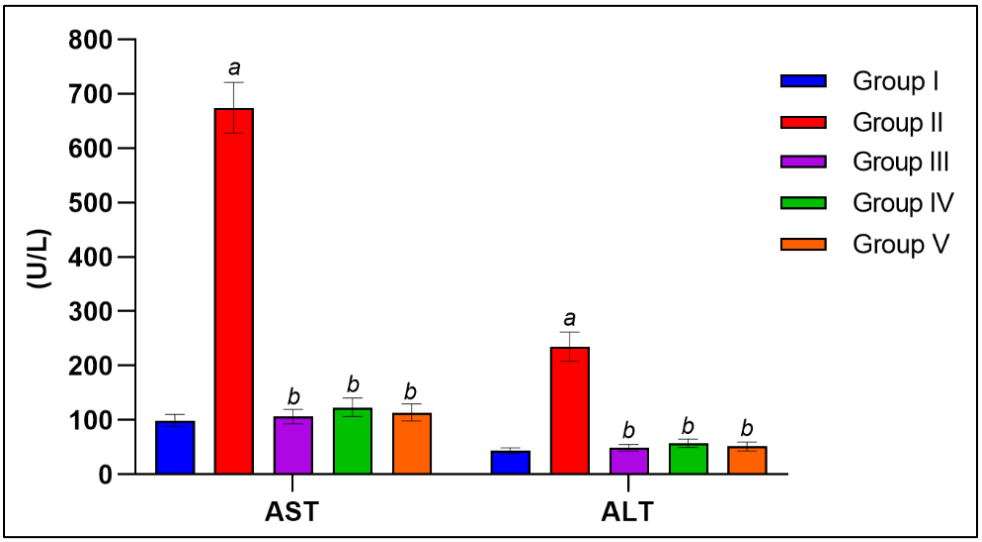


Figure 8.4 Effect of **7** on serum AST and ALT levels of hepatoxicity-induced treatment groups. Group I, Healthy Control; Group II, Disease Control (Paracetamol induced hepatotoxicity); Group III, represented Compound 7 (20 mg/kg); Group IV, represented Silybinin (20 mg/kg); Group V, represented Silymarin (300 mg/kg). Data expressed in Mean ± S.D; $^{a}p < 0.05$ vs. healthy control; $^{b}p < 0.05$ vs. disease control.

The serum of animals was evaluated for alterations in other parameters, viz total cholesterol, triglycerides, and blood glucose levels which are affected by liver impairment. All the parameters were significantly higher in disease-control Group II and fell within normal range in Groups III, IV, and V. The mean serum levels of triglycerides and glucose displayed no statistically significant difference between Group IV and V, but this difference was significant in case of total cholesterol levels. The difference in mean serum levels of all the three parameters in Groups III and V were substantial. There was a significant difference between Group III and IV in case of total cholesterol, but it was approximately equivalent in case of other two parameters, i.e., glucose and serum triglycerides levels. The liver function test of mice in Group III for all the parameters was comparable to Group I (Figure 8.5). The results revealed the protective action of compound **7** against paracetamol-induced hepatotoxicity.

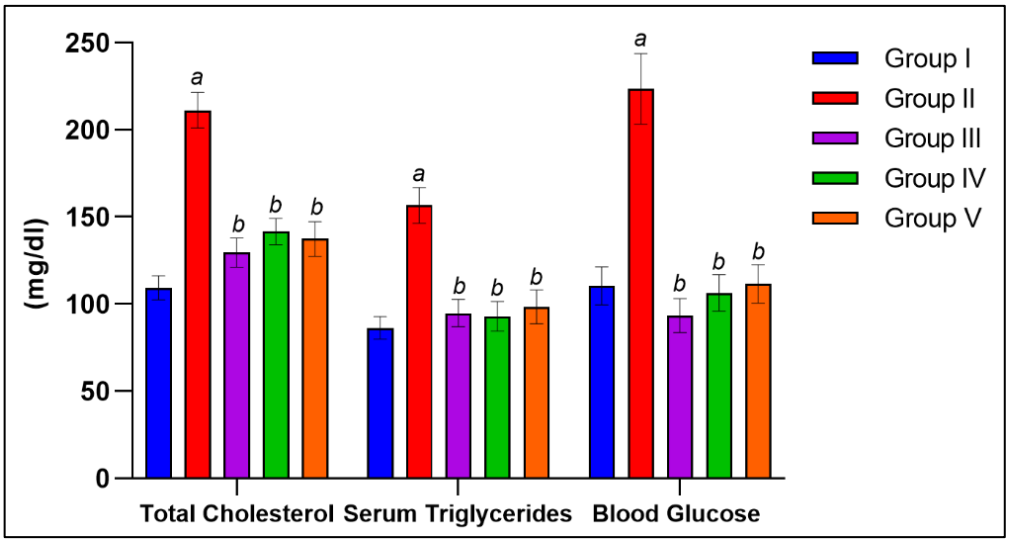


Figure 8.5 Effect of **7** on serum cholesterol, triglycerides, and glucose levels of hepatoxicity-induced treatment groups. Group I, Healthy Control; Group II, Disease Control (Paracetamol induced hepatotoxicity); Group III, represented Compound 7 (20 mg/kg); Group IV, represented Silybinin (20 mg/kg); Group V, represented Silymarin (300 mg/kg). Data expressed in Mean ± S.D; $^{a}p < 0.05$ vs. healthy control; $^{b}p < 0.05$ vs. disease control.

It has been shown that paracetamol causes significant inflammatory penetration in the liver parenchyma and its surrounding tissues. Group II showed disruption in the lobular structure of hepatic tissue due to portal vein inflammation and necrosis of the liver parenchymal cells (Figure 8.6) that was also indicated by amplification in serum levels of liver marker enzymes, i.e., AST and ALT. Groups IV and V showed improved histological changes compared to Group II. Group III showed visible improvement in the lobular structure of hepatic parenchymal tissue and an apparent reduction in inflammation and necrosis, comparable to that in Group I. The histopathological analysis revealed that one week of pretreatment with compound **7** shielded the rats' liver against the histological alterations brought on by paracetamol.

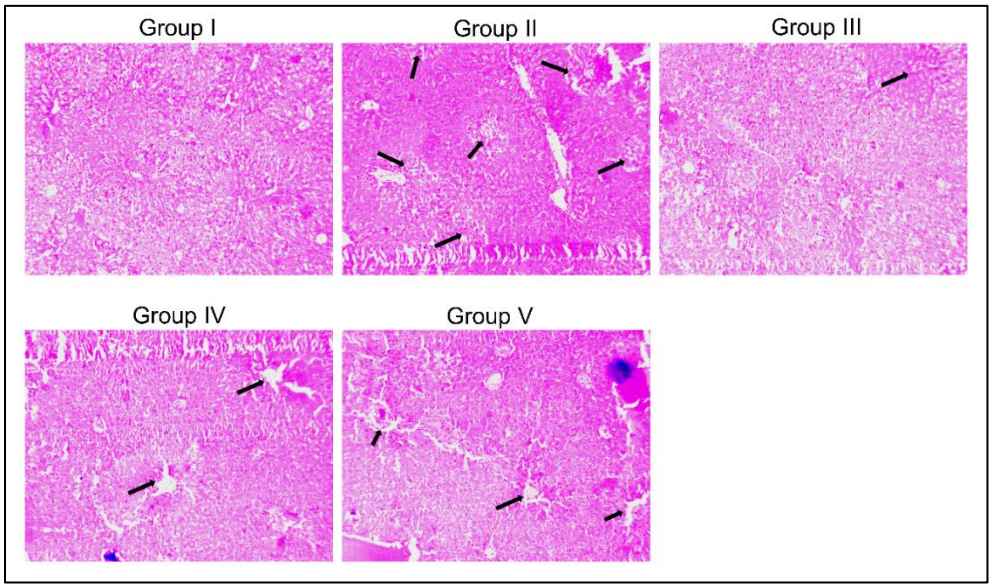


Figure 8.6 Representative pictures showing histopathological effect of compound **7**, silybinin, and silymarin on paracetamol-induced changes in liver tissues.

### 8.3.6 Molecular docking studies

To further strengthen the credibility and reliability of our study, *in silico* docking studies of both the enantiomers of compound **7** (Figure 8.7) and indomethacin was conducted against respective inflammatory cytokines. The interaction table and figure are summarized in Table 8.1 and Figure 8.8. The results of docking studies were in agreement with the *in vitro* results and overall findings of the study. Compound **7** displayed good binding energy with the respective proteins. The docking interaction diagram also revealed that compound **7** interacted with various active site residues. The overall docking results of compound **7** were either better or comparable to indomethacin and the binding was best with IL-8, followed by TNF-α, Il-6, and VEGF.

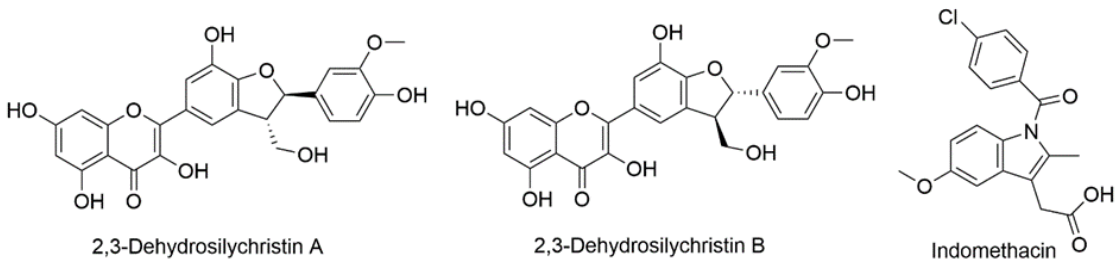


Figure 8.7 Different enantiomers of **7** used for docking studies.

Table 8.1 Interaction table of **7** with inflammatory cytokines.

| **TNF-α (PDB ID: 7JRA, Chain: A)** | | | |
|---|---|---|---|
| **Ligands** | **Binding energy (Kcal $mol^{-1}$)** | **Ligand efficiency (Kcal $mol^{-1}$)** | **Ligand interactions** |
| **2,3-Dehydrosilychristin A** | -8.92 | -0.255 | A:Val 93 (Pi-Alkyl, Pi-Sigma), A:Arg 108 (H-Bond), A:Ala 109 (H-Bond), A:Phe 220 (H-Bond), A:Gly 224 (H-Bond) |
| **2,3-Dehydrosilychristin B** | -7.38 | -0.211 | A:Val 93 (Pi-Alkyl, Pi-Sigma), A:Arg 108 (H-Bond), A:Ala 110 (H-Bond), A:Phe 220 (H-Bond), A:Gly 223 (H-Bond) |
| **Indomethacin** | -8.7 | -0.348 | A:Glu 99 (Pi-Anion), A:Lys 141 (H-Bond & Alkyl), A:Asp 219 (H-Bond & Pi-Anion), A:Phe 220 (H-Bond & Pi-Pi Stacked), A:Ala 221 (Alkyl) |
| **IL-6 (PDB ID: 1ALU, Chain: A)** | | | |
| **2,3-Dehydrosilychristin A** | -6.01 | -0.172 | A:Asn 63 (H-Bond), A:Lys 86 (H-Bond), A:Glu 93 (H-Bond, Pi-Anion), A:Asp 140 (H-Bond) |
| **2,3-Dehydrosilychristin B** | -7.48 | -0.214 | A:Glu 172 (H-Bond, Pi-Sigma), A:Gln 175 (H-Bond), A:Ser 176 (H-Bond), A:Arg 179 (H-Bond, Pi-Cation), A:Arg 182 (H-Bond) |
| **Indomethacin** | -7.62 | -0.305 | A:Leu 64 (H-Bond & Pi-Sigma), A:Lys 66 (Alkyl), A:leu 165 (Alkyl), A:Arg 168 (H-Bond) |
| **IL-8 (PDB ID: 5D14, Chain: A)** | | | |
| **2,3-Dehydrosilychristin A** | -9.09 | -0.260 | A:Lys 9 (Pi-Cation), A:Ile 38 (Pi-Alkyl), A:Glu 46 (H-Bond, Pi-Cation), A:Leu 47 (Pi-Sigma), A:Cys 48 (H-Bond, Pi-Sulfur), |
| **2,3-Dehydrosilychristin B** | -10.12 | -0.289 | A:Lys 9 (H-Bond, Pi-Alkyl, Pi-Cation), A:Tyr 11 (H-Bond, Pi-Pi T-Shaped), A:Glu 46 (H-Bond, Van der Waals), A:Leu 47 (Pi-Sigma), A:Cys 48 (H-Bond, Pi-Alkyl) |
| **Indomethacin** | -10.1 | -0.404 | A:Ile 8 (Pi-Alkyl), A:Lys 9 (H-Bond, Pi-Cation & Pi-Alkyl), A:Leu 47 (Pi-Alkyl), A:Cys 48 (H-Bond & Pi-Sulfur) |
| **VEGF (PDB ID: 1FLT, Chain: V)** | | | |
| **2,3-Dehydrosilychristin A** | -6.66 | -0.190 | V:Cys 61 (H-Bond), V:Asn 62 (H-Bond), V:Cys 68 (H-Bond, Pi-Sulfur), V:His 99 (Pi-Pi T-Shaped), V:Lys 107 (H-Bond) |
| **2,3-Dehydrosilychristin B** | -6.24 | -0.178 | V:Cys 60 (Pi-Sulfur), V:Cys 61 (H-Bond, Pi-Alkyl)), A:Glu 64 (H-Bond), V:Glu 67 (H-Bond, Pi-Anion), V:Cys 68 (H-Bond) |
| **Indomethacin** | -6.14 | -0.246 | V:Ile 35 (Pi-Alkyl), V:Ile 46 (Pi-Alkyl), V:Phe 47 (Alkyl), V:Lys 48 (H-Bond & Pi-Alkyl), |

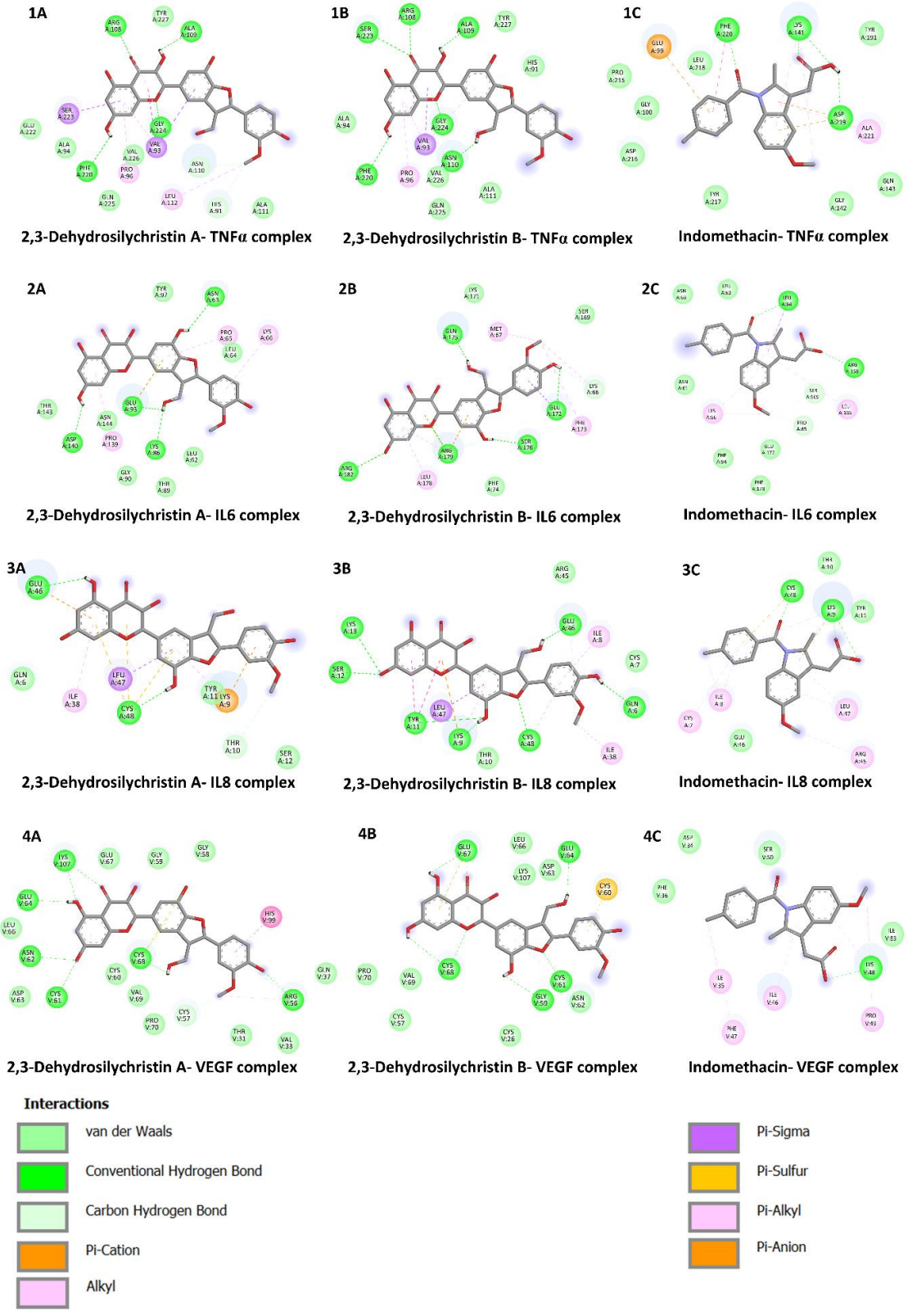


Figure 8.8 Protein-ligand interaction diagram of enantiomers of **7** with different cytokines.

## 8.4 Conclusion

This study reports the presence of silychristin and 2,3-Dehydrosilychristin (**7**) in Nirgundi leaves, expanding the scope of Nirgundi's potential benefits. Compound **7** exhibited potent antioxidant activity, *in vitro* anti-inflammatory and *in vivo* hepatoprotective activities suggesting its significant role in analgesic, anti-inflammatory, and hepatoprotective properties of Nirgundi leaves. The identification of silychristin and isolation of 2,3-Dehydrosilychristin from *V. negundo* opens new avenues to explore it as an alternative source of various flavonolignans. Thus, *V. negundo* could serve as more economical option for large scale extraction of silymarin flavonolignans. Additionally, this provides new prospects for investigating diverse biological potentials of Nirgundi beyond its antioxidant and anti-inflammatory attributes. Based on these findings, it becomes imperative to conduct an in-depth bioprospection study involving different *Vitex* species to discover the prospective flavonolignan and other diverse chemovars for future investigations.